2022

Experimental Study to Enhance the Performance of Li-Fe-Co-Si Active Magnetic Regenerator for Room Temperature Cooling Applications

Priya Singh

Kavita Srikanti

Manish Chandra

R Gopalan

Satyanarayanan Seshadri

An Experimental Study on Performance of Li-Fe-Co-Si Active Magnetic Regenerator for Room Temperature Cooling Applications

Priya SINGH[1], Kavita SRIKANTI[2], Manish CHANDRA[1], R. GOPALAN[2], Satyanarayanan SESHADRI[1*]

[1]Energy and Emissions Research Group (EnERG Lab), Department of Applied Mechanics,
Indian Institute of Technology Madras,
Chennai, Tamil Nadu, India
Phone: +91-9845068998, satya@iitm.ac.in

[2]Centre for Automotive Energy Materials, International Advanced Research Centre for Powder Metallurgy and New Materials,
Chennai, Tamil Nadu, India
Phone: +91-9962052712, srikanti.kavita@gmail.com

* Corresponding Author

ABSTRACT

The need to shift towards environmentally benign cooling technologies has increased due to nearly 8% of global greenhouse gas emissions coming from conventional refrigeration systems based on vapor compression technology. The existing vapor compression-based cooling technology is mature in many aspects, but it has adverse environmental impacts. A magnetic refrigeration system (MRS) is emerging as one of the best alternatives to conventional refrigeration systems due to its negligible ozone depletion potential and low global warming potential. Magneto-caloric materials (MCM) are the core component of this technology due to their property to become hot on magnetization and cold when demagnetized. The magnetic refrigeration system is analogous to the conventional vapor compression refrigeration system. The heating and cooling on demagnetization of solid refrigerant MCM are like compression and expansion of gas refrigerants. Many compounds are classified as MCM, among which the La-Fe-Co-Si group of MCM is earth abundant and works near ambient temperatures (15 – 25 °C). The second component of MRS is the magnet, and for this study, we chose the nested Halbach magnet array (1.5 T). We selected the comb-shaped geometry of La-Fe-Co-Si MCM with an area-to-volume ratio of 4.5 for efficient heat transfer. La-Fe-Co-Si group of MCM contains Fe, making it prone to corrosion, limiting our choice of heat transfer fluids to non-aqueous. A hydrocarbon heat transfer fluid was thus used to evaluate the MCM array's performance in this study. A slotted tray consisting of MCM blocks inside a cylindrical tube and heat transfer fluid forms the Active Magnetic Regenerator (AMR). MCM blocks are cascaded in AMR cylinder with respective curie temperatures (in °C) in the following order 10.9, 12.9, 14.9, 16.9, 18.9, 20.9, 24.9, and 26.9. A reciprocating system is chosen for this configuration to reduce power consumption. From our observations, 10 watts of refrigeration capacity is achievable with this configuration. For the frequency range of 2.8mHz and 75mHz, the temperature span achieved is nearly 0.85K for 0.5 lit/min of HTF flow rate. The specific refrigeration capacity was 6.29K/kg of solid refrigerant La-Fe-Co-Si MCM. The cooling capacity and temperature span of MRS were dependent on the rate of change of magnetic flux across the MCM affected by moving it in and out of the magnetic field and on the response time for heat transfer. The study helped to optimize the heat transfer in AMR by tuning of frequency and flow rate for this system.

1. INTRODUCTION

Refrigeration has become an essential part of 21st-century life. This “invisible” industry plays a significant role in numerous sectors ranging from food processing, manufacturing to entertainment and healthcare. The current global trend shows that demand for room temperature refrigeration systems increases substantially with improving living

standards and population growth. Today's electricity consumption for air conditioning and refrigeration systems is about 2000 TWh, accounting for nearly 20% of the global electricity consumption. It is anticipated to triple by 2050 by International Energy Agency (International Energy Agency (IEA), 2018)(Coulomb, Dupont, & Pichard, 2015). Vapor-compression systems (VCS) are regarded as a reliable technology with optimized production, maintenance, cost, and safety to fulfil the demand for refrigeration & air-conditioning. However, the refrigerants used in VCS have high global warming potential (GWP) and ozone depletion potential (ODP), causing an adverse ecological effect, and up to 8% of global greenhouse gas emission (International Institute of Refrigeration, 2017).

This situation has driven the development and search for alternative refrigeration means that are environmentally friendly, more efficient, and can serve the demand. The magnetic refrigeration system (MRS) is emerging as one of the best alternatives to the conventional refrigeration system(Gschneidner Jr & Pecharsky, 2008). MRS has a potentially high coefficient of performance, 30%-60% of Carnot efficiency (Zimm et al., 1998), and can use solid refrigerants with negligible GWP and ODP(Aprea, Greco, Maiorino, & Masselli, 2015).

Magnetic refrigeration technology is based on the magneto-caloric effect (MCE), a characteristic present in all magnetic materials and alloys. By varying the intensity of the magnetic field on the material, the MCE manifests as a temperature change, which can be used for developing a cooling system. They represent a significant niche for magnetic cooling technologies due to their potential to outperform traditional vapor compression systems. For the last two decades, nearly 80 prototypes of MRS for room temperature applications have been built and reported (Yu, Liu, Egolf, & Kitanovski, 2010)(Greco, Aprea, Maiorino, & Masselli, 2019). However, they have not reached a point when they can be used for everyday refrigeration and air conditioning demands (Tušek et al., 2020). The reason for non-success is inadequate cooling capacity and temperature span. The temperature span of an MRS prototype depends on the amount of adiabatic temperature change in MCM and heat transferred to the heat transfer fluid (HTF). A high adiabatic temperature change of the MCM yields a greater temperature span of the prototype. The adiabatic temperature change increases with the magnetic flux change across MCM (Magnus et al., 2005). However, there is a limitation in the magnetic field intensity of the permanent magnet. Also, most magnetic materials have very small adiabatic temperature changes ranging from 2-3K at their respective curie temperature (for a 1.5 Tesla change in magnetic induction).

When magnetic materials are used as an active magnetic regenerator, the temperature span can be increased several times over the adiabatic temperature change (Barclay & Steyert, n.d.). For this reason, the active magnetic regenerative (AMR) cycle is the standard operative cycle of permanent magnet room-temperature devices(Tušek et al., 2020). Availability of Gd is scarce in nature; this makes MRS based on Gd economically unscalable for large-scale production(Nikly & Muller, 2007). This paves the way for La-Fe-Co-Si-based MCMs to emerge in the magnetic refrigeration domain as an alternative to Gd-based MCMs. Lionte et al. have presented the basis for applying first-order La-Fe-Co-Si-based alloys in MRS(Lionte, Barcza, Risser, Muller, & Katter, 2021). La-Fe-Co-Si-based alloys have only a tiny fraction of Lanthanum by composition. This brings down the material cost, which is critical for scalable production. Our study focuses on La-Fe-Co-Si-based MCM due to significantly higher adiabatic temperature change and tuneability of its Curie temperature(Fujita, Akamatsu, & Fukamichi, 1999). In this paper, we have done an experimental study using a multilayer AMR in which MCM is cascaded in the increasing order of Curie temperature to enhance magnetic refrigeration (MR) temperature span. However, Li-Fe-Co-Si MCM corrodes when there is direct contact with aqueous fluid. So, we have chosen a hydrocarbon-based non-aqueous fluid with properties similar to Aviation Kerosene for HTF. Presently, no research studies have used this fluid as HTF in MRS. We have studied the temperature span achieved by varying the operating frequency of MRS. Our study uses permanent magnets limited by magnetic field intensity but provides higher energy efficiency.

2. EXPERIMENT DESCRIPTION

2.1 Magneto-caloric Material and Construction of AMR

For an MCM with a second-order phase transition, the adiabatic temperature change and isothermal entropy change can be calculated using the following equations (Kitanovski & Egolf, 2006).

$$\Delta T_{ad} = -\mu_o \int_{H_1}^{H_2} \frac{T}{C_h} \left(\frac{\delta M}{\delta T}\right)_H dH \quad (1)$$

$$\Delta s_M = \mu_o \int_{H_1}^{H_2} \left(\frac{\delta M}{\delta T}\right)_H dH \quad (2)$$

The isothermal entropy change indicates the cooling capacity of a magneto-caloric refrigerant, and the adiabatic temperature change indicates the temperature span. Information about adiabatic temperature change is important to know the material's usability for refrigeration devices. Temperature span is supposed to be achieved in cooling technologies. Moreover, considering that the heat transfer between the material and the working fluid is irreversible, a significant adiabatic temperature change is required to overcome the irreversible heat losses. To obtain this a large surface area for heat transfer, the comb-shaped geometry of MCM was chosen. This provided area to volume ratio ≈ 4.5. The front view and dimension of the specimen are shown in Figure 1.

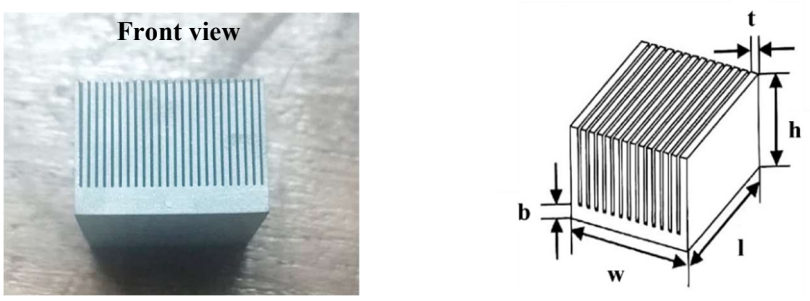

Figure 1: (a) Photograph of front view comb-shaped specimen, (b) Dimension definition of specimen where, base(b)=1.5mm, width(w)= 15mm, length(l)= 20mm, height(h)=10mm and thickness(t)=0.4mm.

The material was procured from Vacuumschmelze Gmbh & Co. Kg. produced using powder metallurgy (reactive sintering method). The material is commercially known as Calorivac C. The technical datasheet of the material provides specific isothermal entropy change for a typical Calorivac C alloy for 1.5 T magnetic induction change as shown in Figure 2. This relationship between entropy changes and ambient temperature is linear, with a slope of 0.717 and an intercept of 261.607.

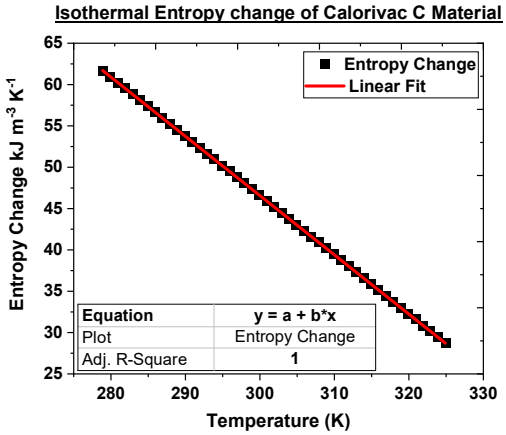

Figure 2: Isothermal entropy change of a typical Calorivac C material with temperature at $\Delta B_{ext} = 1.5T$.

The entropy change is decreasing with an increase in ambient temperature around MCM. Magnetic material is used as a refrigerant as well as a regenerator. The active magnetic regenerator (AMR) is a closed circuit consisting of magnetic material and HT fluid. In the Figure 3(a) shows the front view of active magnetic regenerator used in the experimental setup and Figure 3(b) shows the schematic of active magnetic regenerator transverse view, each MCM blocks are place in the increasing order of their Curie temperature. In the active magnetic regenerative cycle, the magnetic material serves as a refrigerant providing temperature change due to adiabatic magnetization or demagnetization and as a regenerator for the heat transfer fluid and temperature change is measured using thermistor T1 and T2 placed beneath the first and last MCM respectively.

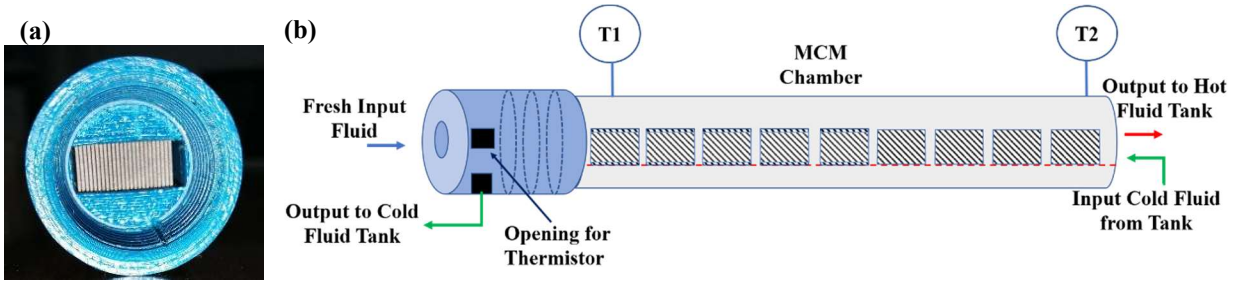

Figure 3: (a) Front view of active magnetic regenerator, (b) Schematic of Active Magnetic Regenerator (AMR).

The AMR cycle consists of four steps, illustrated in Figure 4 as a flow chart (Egolf, Kitanovski, Vuarnoz, Diebold, & Besson, 2006). The flow chart of magnetic refrigeration system and processes are compared to vapour compression refrigeration system Magnetic refrigeration system consists of four steps: Magnetization: the MCM in the AMR is magnetized, causing the temperature to increase, Cold blow: HTF flows from cold end to hot end, passing through channels in the now-hot parallel plate AMR, Demagnetization: the MCM in the AMR is demagnetized, causing the temperature to decrease, Hot blow: HFT flows from hot end to cold end, passing through channels in the now-cold parallel plate AMR. The steps are analogous to a conventional vapor compression system that is compression, heat rejection, and expansion, and heat addition.

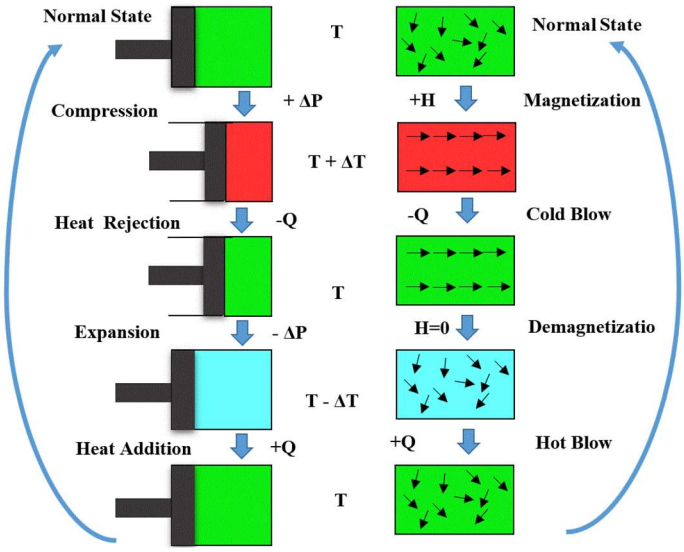

Figure 4 Flow chart of Magnetic Refrigeration System (MRS).

Our setup of AMR consists of 9 blocks of varying material compositions to have increasing Curie temperatures (in °C) as 10.9, 12.9, 14.9, 16.9, 18.9, 20.9, 24.9, and 26.9, respectively. Each block is of dimension 20mm by 15mm by 10 mm and has 25 plates, each with a plate thickness of 0.4mm and spacing 0.2 mm between consecutive plates. The total length of AMR is 18 cm. Each material has a maximum magneto-caloric effect of nearly 2.5K for a magnetic field change of 1.5 T at its respective Curie temperature. Figure 5 shows the MCMs Curie temperature (T_c) and their adiabatic temperature change of each MCM block for magnetic intensity change of 1.5 T at different temperatures, and it is highest at its respective Curie temperature. The graph presented here is plotted from the technical data sheet of MCM provided by Vacuumschmelze Gmbh & Co. Kg. The mass and volume of each block are 15g and 2150 mm^3, respectively. These materials exhibit a first-order magnetic phase transition, characterized by a very narrow and sharp entropy change as a function of temperature. Our apparatus can reach as low as 8.4 °C and as high as 29.4 °C. The enthalpy changes of 9 materials approximated together is calculated using the entropy value of the materials using Equations (3) (Kitanovski et al., 2015). The specific heat capacity of La-Fe-Co-Si-MCM is 900J/Kg K (Bjørk, Bahl, & Katter, 2010).

$$dq = dh = T\left(\frac{\delta s}{\delta T}\right)_H dT \tag{3}$$

MCMs Curie Temperature(T_c) and their adiabatic temperature change with operating temperature

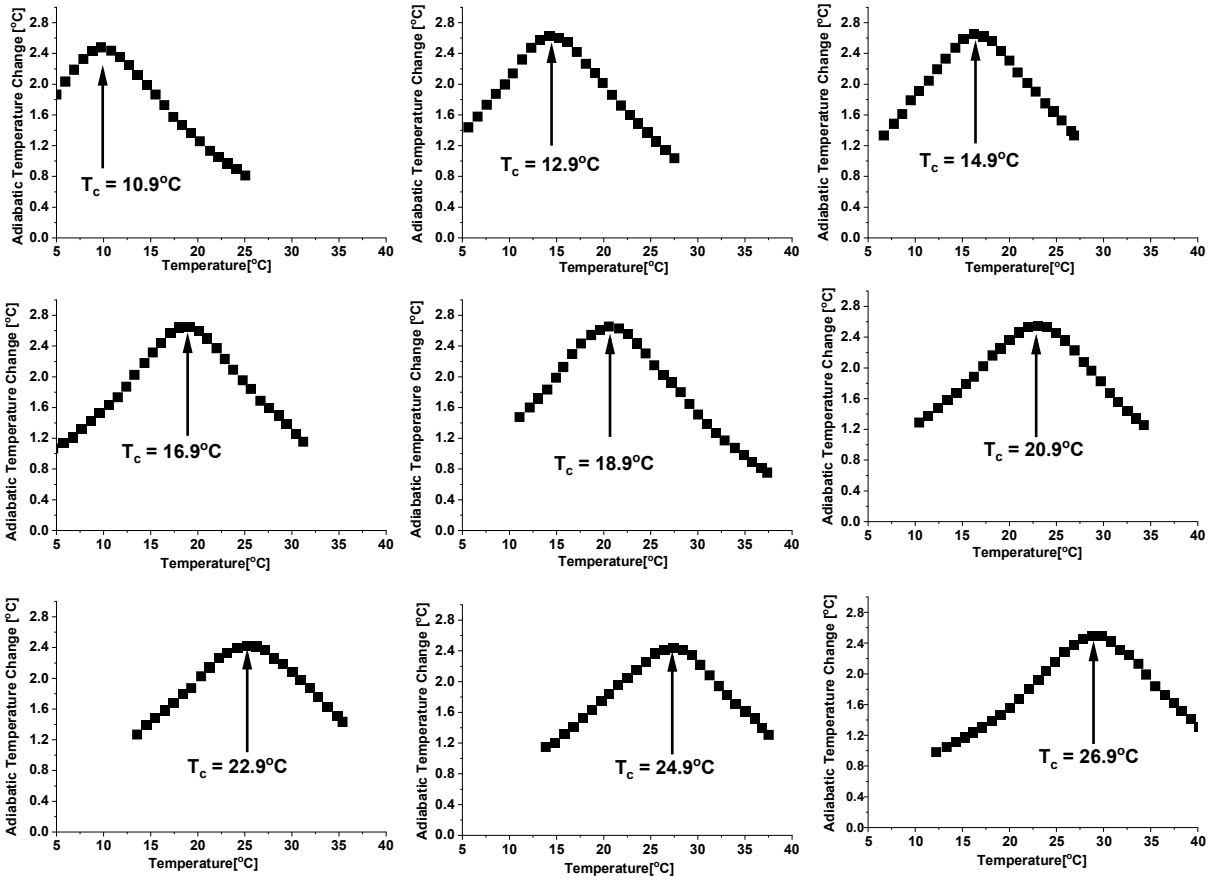

Figure 5: The Curie temperature and their adiabatic temperature change of nine different MCMs blocks.

We have used a Halbach cylinder consisting of 8 blocks of permanent magnets to avoid consuming energy for producing a magnetic field. The cylinder has an inner radius of 12 mm, an outer radius of 50 mm, and a length of 250 mm. The volume of the high flux density region, i.e., the cylinder bore, is 1.13 x 10^{-3} lit. The magnetic field intensity is plotted and validated using instruments at the Centre for Automotive Energy Materials, ARCI, Chennai (IITM Research Park) shown in Figure 6. In the graph, simulation and the actual results for magnetic intensity profile follows similar trend.

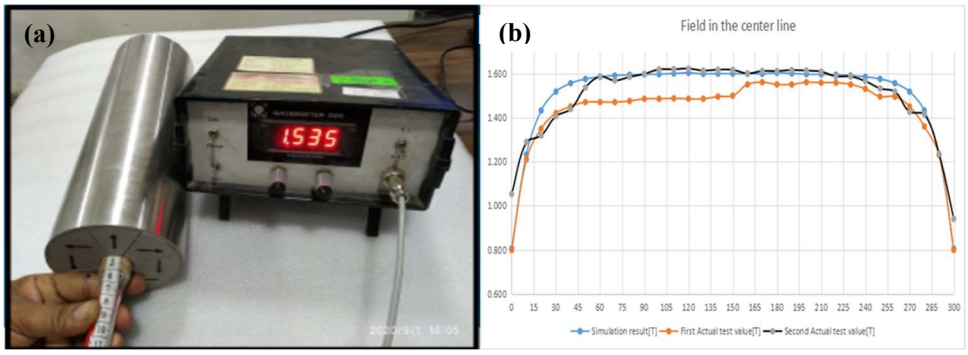

Figure 6: (a) Halbach array magnetic field intensity being validated (b) Halbach array intensity measurement.

The heat-transfer (working) fluid and its thermo-hydraulic properties have an essential role in the performance of the AMR. To ensure good cooling characteristics at a high frequency (> 50mHz) of operation, the applied working fluid should have high thermal conductivity, high thermal diffusivity, and a low viscosity. The majority of the magnetic

refrigerator prototypes use water-based heat transfer fluids with different alcohol additives. Some earlier prototypes also applied gases, such as helium, nitrogen, or air(Gao et al., 2016). Water is often chosen due to its excellent heat transfer properties, non-toxicity, and simplicity of use. Our experimentation showed that using a typical HTF-like water-alcohol mixture (2:1 ratio) corrodes our MCM sample instantaneously.

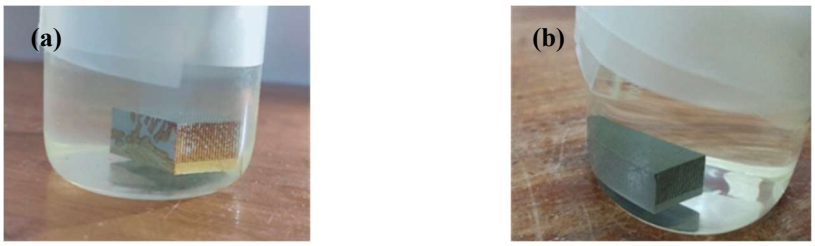

Figure 7: (a) Image of MCM immersed in water-alcohol mixture (b) Image of MCM immersed in Cal 77.

Figure 7(a) shows the image of our specimen taken within 2 minutes after immersion. Zhang et al. describe that the corrosion of La-Fe-Co-Si MCM decreases the mass of the matrix phase, decreasing the maximum magnetic entropy change of the compound(Zhang, Long, Ye, & Chang, 2011). Using hydrocarbon-based non-aqueous fluid (commercially known as Cal 77) showed no corrosion. The viscosity and density of the HTF (Cal 77) were experimentally determined to be 1.562 mPa.s and 774 Kg/m^3 at 28°C, respectively. It has a specific heat capacity of 2.01 kJ/kg/K and a conductivity of 0.145 W/mK. Even after a week of immersing the material in Cal 77, there was no corrosion seen (Figure 7b). Here, pressurized gases cannot be used due to the fragility of the design of the MCM block.

2.2. Apparatus description

There are two main types of MRS in the literature based on the relative motion between the magnet and magnetic material: reciprocating type and rotating type. We choose the reciprocating type as it consumes lesser power and is more robust. The reciprocating system consists of the AMR and the Halbach array. The reciprocating motion is provided using a compressor, proportional pressure regulating valve (PPRV), and pneumatic piston. By regulating pressure, PPRV controls the speed, and the solenoid valve changes the direction of piston movement. The experimental setup of magnetic refrigeration system is shown in Figure 8.

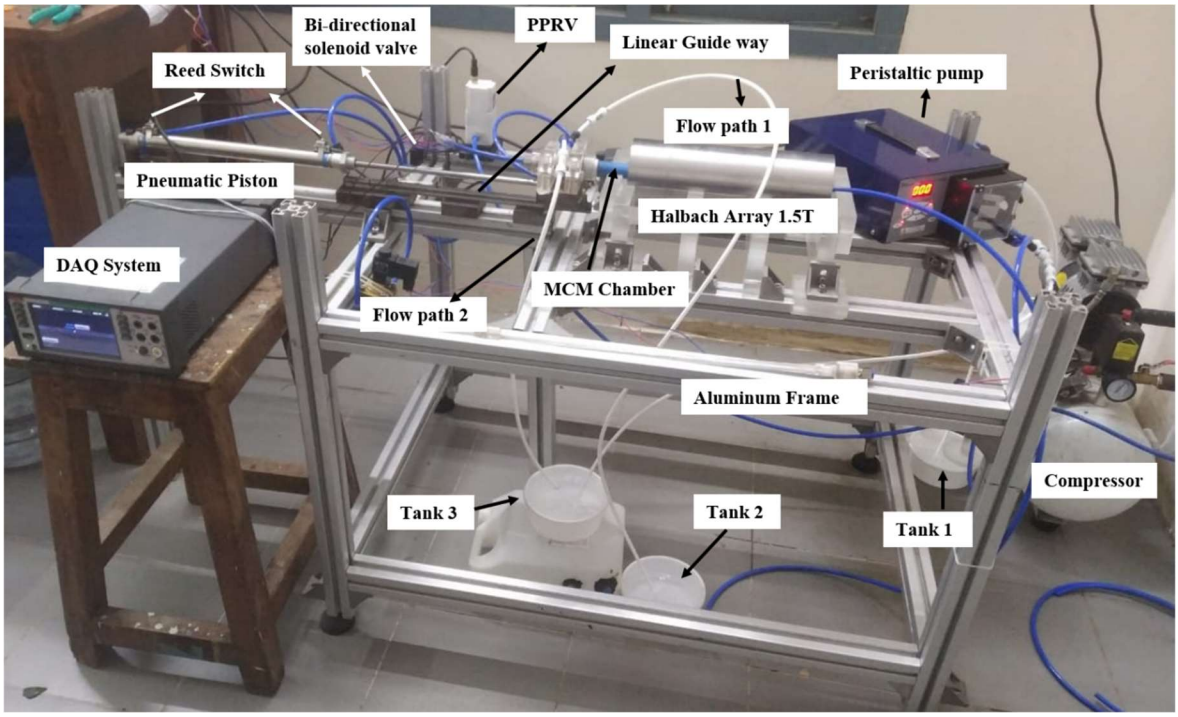

Figure 8: Magnetic Refrigeration system experimental setup.

The system consists of two separate HTF flow paths (FP-1 and FP-2), which are both non-mixing and non-heat exchanging. The flow of HTF in one cycle is as follows: At first, MCM magnetizes, and HTF flows (in FP-1) from tank-1, which is maintained at ambient temperature, to tank-2 through AMR, in effect, cooling it. Next, when MCM demagnetizes, a separate bulk of HTF circulates (in FP-2) from tank-3 through AMR back to tank-3, making it colder every cycle. The hydraulic system consists of inline piping, the non-return valve, and a peristaltic pump to control the fluid flow bi-directionally. The measurement system consists of thermistors connected to the base of 3 of the 9 MCM blocks (the first block, the last block, and the middle block). Data is logged using a DAQ. Reed switches are used to sense and control the position of the piston end in order to change the direction when the piston reaches the dead ends. All the systems are connected and programmed on a microcontroller. The outer frame of the apparatus is made out of extruded aluminium.

3. RESULTS AND DISCUSSION

As discussed in section 2.1, the appropriate heat transfer fluid was examined using experimentation with water, water-alcohol mixture, and hydrocarbon fluid (Cal 77). Cal 77 properties are calculated using calibrated instruments from the facility at National Centre for Combustion Research and Development (NCCRD), IIT Madras. Cal 77 is similar to aviation fuels in thermo-hydraulic properties. Its flash point is greater than 313K, so it is safe to use in our study, which operates below 303K. After HTF is finalized, a thorough quantitative calculation is done to find the enthalpy change of material on magnetization and demagnetization. With the help of isothermal entropy change data of MCM blocks, we calculated the total enthalpy change of nine MCM blocks as a function of ambient temperature while undergoing a magnetic field change of 1.5T using equation (3). Since isothermal entropy change decreases with rising ambient temperature, the enthalpy changes decrease simultaneously. The trend of enthalpy changes at a given ambient temperature for a magnetic field change of 1.5T is shown in Figure 9.

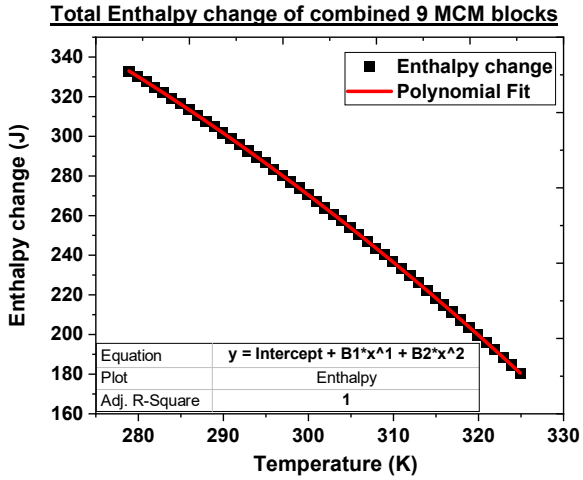

Figure 9: The plot of enthalpy changes of nine MCM blocks with the change of ambient temperature.

This graph shows a decreasing trend with the increase in ambient temperature. In our study, the starting temperature is 300K to 302K, so enthalpy change varies between 245-260 J. At 280K ambient temperature, the enthalpy change obtained is 332 J, the maximum heat that can be transferred (absorbed or released by MCM). The relation between enthalpy changes and ambient temperature is quadratic with an equation of $y = -0.012x^2 + 5.062x - 4.11$. The theoretical temperature change in the magnetization and demagnetization process of material is calculated using equation (4). The fluid flow rate is 0.495lit/min, and the specific heat capacity is 900J/kgK. The theoretical temperature change as a function of ambient temperature is shown in the graph in Figure 10(a). The experimental setup operates in the temperature range from 281K to 301K. The maximum theoretical temperature change of MCM achieved by the apparatus is 2.6 K.

$$\Delta T = \frac{dq}{\dot{m}c} \tag{4}$$

Assuming complete heat transfer from material to HTF, the theoretical refrigeration capacity is calculated considering the flow rate of HTF to be 0.495 lit/min. The variation in the refrigeration capacity with the ambient temperature change is shown in Figure 10(b). the graph shows the decreasing trend because the amount of heat absorbed during demagnetization is temperature-dependent. Theoretically, the maximum refrigeration capacity achievable is 34.3W from the given system.

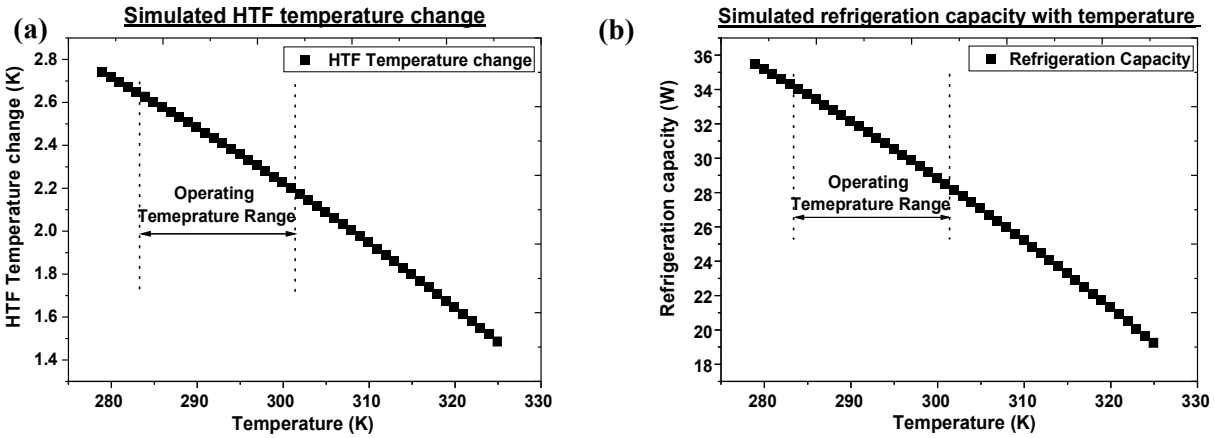

Figure 10: (a) Simulated HTF temperature change, (b) Simulated HTF refrigeration capacity variation, of combined nine MCM materials blocks with operating temperature at $\Delta B_{ext} = 1.5T$.

Experiments were conducted for two sets of frequency. In the first set, the operating frequency was 75mHz, the initial temperature was 27.93 °C, the highest recorded temperature during magnetization was 28.04 °C, and the lowest temperature recorded after demagnetization was 27.70 °C. The temperature span achieved was 0.34 °C, the drop in temperature of HT fluid from ambient was 0.23 °C, and the overall refrigeration capacity achieved was 2.94W. In the second set, the operating frequency was 2.8mHz, the initial temperature was 27.70 ° C, the highest recorded temperature during magnetization was 27.9 ° C, the lowest temperature recorded after demagnetization was 26.85 ° C. The temperature span achieved was 1.05 ° C, the drop in temperature of HT fluid from ambient was 0.85 °C, the overall refrigeration capacity achieved was 11W, and the system efficiency was 40%. The achieved temperature span was lower than theoretical estimates as it was difficult to maintain adiabatic condition throughout the process. The flow rate of HTF is kept fixed at 383.13 g/min (0.495 lit/min) during both sets. Heat capacity HT ($\dot{m}C_{pHTF}$) = 12.83 W K^{-1}. The temperature versus time variation of the heat transfer fluid of thermistor T1 and T2 with high and low frequency of movement of MCM chamber is shown in Figures 11(a) and 11(b), respectively.

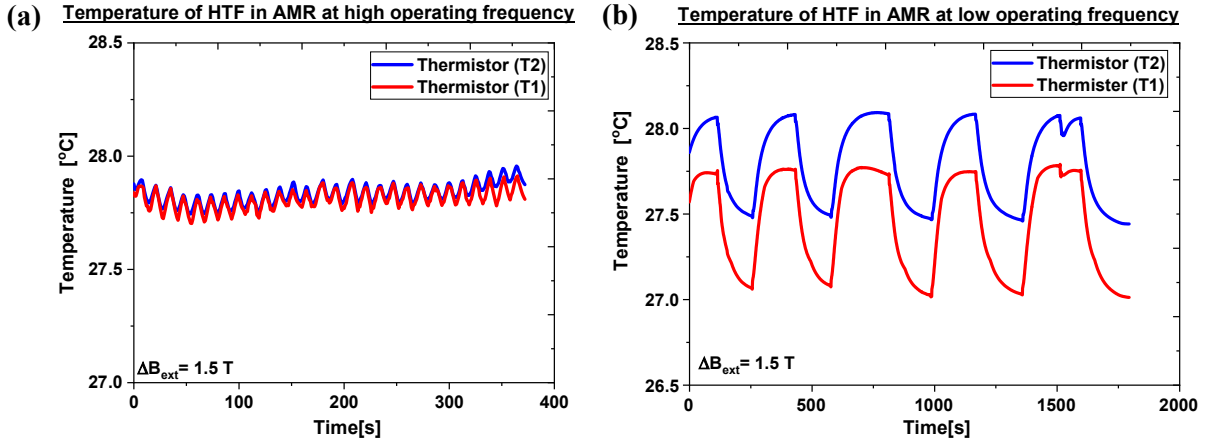

Figure 11: (a)High frequency, (b) low frequency movement of MCM chamber.

The possible reason behind the temperature difference at both thermistor T1 and T2 is the mixing of HTF with the cold and hot side fluid. As a result, cold side thermistor T1 shows a lower temperature than T2. The comparison of cooling

efficiencies of AMR at MCM chamber movement frequency is shown in Figure 12, the cooling efficiency in lower operational frequency is 75% higher than that in the higher movement frequency of MCM chamber.

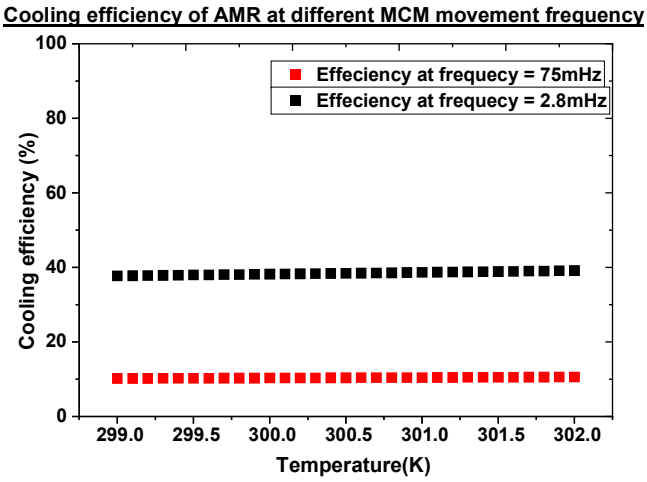

Figure 12: Comparison of cooling efficiencies at different movement frequency of MCM chamber.

The heat transfer from MCMs to the HTF takes some amount of time and due to that cooling efficiency increases once the operational frequency is low. At the higher frequency of operations, HTF did not get enough time to absorb or transfer heat to the MCMs and resulting into lower cooling efficiency.

4. CONCLUSION

Our work has prototyped a La-Fe-Co-Si-based alloy as MCM and Hydrocarbon as HTF in a magnetic refrigeration system. The Cal 77 selected as HTF and operated at 0.495 lit/min flow rate, two frequencies (75mHz and 2.8mHz), and 28 °C ambient temperature in the MRS. Frequency constraints devices heat exchanging efficiency when high and its cooling capacity when low. Despite the lower specific heat capacity of Cal 77 compared to water, heat transfer performance was found to be decent as the device approached 40 percent of efficiency. This work contributes toward the realization of a magnetic refrigeration system using linearly moving AMR and a static magnetic field. The current setup gives a cooling capacity of ≈ 11 W at room temperature. The temperature span achieved has been noted to be 1.05 °C in the current operating condition. The measured temperature span lower than expected due operational system limitations firstly, not able to maintain adiabatic conditions during operations and secondly, hot and cold fluid mixing in tube during movement change of MCM chamber. Analysis of performance in the temperature-controlled chamber, varying the initial temperature, and varying the flow rate are subject to future publications

NOMENCLATURE

Symbol	Description	Unit
ΔT_{ad}	adiabatic temperature change	(K)
μ_o	magnetic permeability of free space	$(VsA^{-1}m^{-1})$
M	magnetization	(Am^{-1})
T	magnetic flux density	$(\mathrm{kgs}^{-2}\mathrm{A}^{-1})$
c	specific heat capacity	$(Jm^{-3}K^{-1})$
H	magnetic field intensity	(Am^{-1})
Δs	specific entropy change	$(\mathrm{Jm}^{-3}\mathrm{K}^{-1})$

REFERENCES

Aprea, C., Greco, A., Maiorino, A., & Masselli, C. (2015). Magnetic refrigeration: An eco-friendly technology for the refrigeration at room temperature. Journal of Physics: Conference Series, 655(1).

Barclay, J.A., & Steyert, W.A. (Jun 1982). *Active magnetic regenerator* .US patent document 4,332,135/A/.

Bjørk, R., Bahl, C. R. H., & Katter, M. (2010). Magnetocaloric properties of LaFe13-x-yCoxSi y and commercial grade Gd. *Journal of Magnetism and Magnetic Materials*, *322*(24), 3882–3888.

Coulomb, D., Dupont, J.-L., & Pichard, A. (2015). *The Role of Refrigeration in the Global Economy-29. Informatory Note on Refrigeration Technologies*.

Egolf, P. W., Kitanovski, A., Vuarnoz, D., Diebold, M., & Besson, C. (2006). An introduction to magnetic refregiration. *University of Applie Science of Western Switzerland*, 1–8.

Fujita, A., Akamatsu, Y., & Fukamichi, K. (1999). Itinerant electron metamagnetic transition in La (Fe x Si 1− x) 13 intermetallic compounds. *Journal of Applied Physics*, *85*(8), 4756–4758.

Gao, X. Q., Shen, J., He, X. N., Tang, C. C., Li, K., Dai, W., … Wu, J. F. (2016). Improvements of a room-temperature magnetic refrigerator combined with Stirling cycle refrigeration effect. *International Journal of Refrigeration*, *67*, 330–335.

Greco, A., Aprea, C., Maiorino, A., & Masselli, C. (2019). A review of the state of the art of solid-state caloric cooling processes at room-temperature before 2019. *International Journal of Refrigeration*, *106*, 66–88.

Gschneidner Jr, K. A., & Pecharsky, V. K. (2008). Thirty years of near room temperature magnetic cooling: Where we are today and future prospects. *International Journal of Refrigeration*, *31*(6), 945–961.

International Energy Agency (IEA). (2018). *"The Future of Cooling Opportunities for energy- efficient air conditioning"International Energy Agency Website: www.iea.org, 2018*. Retrieved from www.iea.org

Kitanovski, A., Tušek, J., Tomc, U., Plaznik, U., Ožbolt, M., & Poredoš, A. (2015). *Magnetocaloric energy conversion - From theory to applications*.

Kitanovski, Andrej. (2020). Energy Applications of Magnetocaloric Materials. *Advanced Energy Materials*, *10*(10).

Kitanovski, Andrej, & Egolf, P. W. (2006). Thermodynamics of magnetic refrigeration. *International Journal of Refrigeration*, *29*(1), 3–21.

Lionte, S., Barcza, A., Risser, M., Muller, C., & Katter, M. (2021). LaFeSi-based magnetocaloric material analysis: Cyclic endurance and thermal performance results. *International Journal of Refrigeration*, *124*, 43–51.

Magnets, P. (n.d.). *Permanent Magnets Vacodym • Vacomax Advanced Materials – the Key To Progress*.

Magnus, A., Carvalho, G., Alves, C. S., De Campos, A., Coelho, A. A., Gama, S., … Oliveira, N. A. (2005). The magnetic and magnetocaloric properties of Gd 5Ge 2Si 2 compound under hydrostatic pressure. *Journal of Applied Physics*, *97*(10), 1–4.

Nikly, G., & Muller, C. (2007). Technical and economical criteria to design and realize a magneto-caloric heat pump. *Proceedings of the 2nd International Conference of Magnetic Refrigeration at Room Temperature, Portoroz, Slovenia*, 59–70.

Tušek, J., Kitanovski, A., & Poredoš, A. (2013). Geometrical optimization of packed-bed and parallel-plate active magnetic regenerators. International Journal of Refrigeration, 36(5), 1456–1464.

Tušek, J., Kitanovski, A., Tomc, U., Favero, C., Poredoš, A., Brown, G. V., Wang, H. S. (2020). Review on the developments of active magnetic regenerator refrigerators – Evaluated by performance. *Renewable and Sustainable Energy Reviews*, *133*(1), 110247.

Yu, B., Liu, M., Egolf, P. W., & Kitanovski, A. (2010). A review of magnetic refrigerator and heat pump prototypes built before the year 2010. *International Journal of Refrigeration*, *33*(6), 1029–1060.

Zhang, M., Long, Y., Ye, R., & Chang, Y. (2011). Corrosion behavior of magnetic refrigeration material La–Fe–Co–Si in distilled water. *Journal of Alloys and Compounds*, *509*(8), 3627–3631.

ACKNOWLEDGEMENT

The authors thank Director, ARCI, and Prof G Sundararajan, Distinguished Scientist, ARCI for their keen interest and support in this work. The authors are thankful to the Department of Science and Technology, Government of India, for financial support (No. AI/1/65/ARCI/2014).